Available online at www.sciencedirect.com
ScienceDirect
Journal of Sound and Vibration 323 (2009) 475–493
JOURNAL OF SOUND AND VIBRATION
www.elsevier.com/locate/jsvi

Crowd–structure interaction in footbridges: Modelling, application to a real case-study and sensitivity analyses

Luca Bruno*, Fiammetta Venuti

Politecnico di Torino, Department of Structural Engineering and Geotechnics, Viale Mattioli 39, I-10125 Torino, Italy

Received 23 May 2008; received in revised form 3 December 2008; accepted 3 December 2008
Handling Editor: C.L. Morfey
Available online 20 January 2009

Abstract

A mathematical and computational model used to simulate crowd–structure interaction in lively footbridges is presented in this work. The model is based on the mathematical and numerical decomposition of the coupled multiphysical nonlinear system into two interacting subsystems. The model was conceived to simulate the synchronous lateral excitation phenomenon caused by pedestrians walking on footbridges. The model was first applied to simulate a crowd event on an actual footbridge, the T-bridge in Japan. Three sensitivity analyses were then performed on the same benchmark to evaluate the properties of the model. The simulation results show good agreement with the experimental data found in literature and the model could be considered a useful tool for designers and engineers in the different phases of footbridge design.

1. Introduction

Over the last few decades, several footbridges have shown great sensitivity to human induced vibrations in the lateral direction (e.g. Refs. [1,2]). This phenomenon, known as synchronous lateral excitation, can take place any time pedestrians walk on a surface that oscillates laterally with a frequency that is close to the mean lateral walking frequency (around 1 Hz). When a pedestrian walks on a laterally moving surface, in an attempt to maintain balance, he walks with his legs more widespread and adapts his frequency to that of the moving surface, that is, he synchronises to the structure. Hence, the lateral motion of the upper part of the torso increases and the resulting lateral force increases in turn. This phenomenon is amplified if the pedestrian walks in a crowd, since synchronisation among pedestrians increases the effects of pedestrian–structure synchronisation.

The synchronous lateral excitation phenomenon has never caused structural failure since it is self-limited, that is, when the vibrations exceed a limit value, pedestrians stop walking or touch the handrails, and this causes the vibration to decay. Nevertheless, the resulting reduced comfort for the users has often led to a temporary closure of the footbridge, with consequent economic and social repercussions. In order to avoid this kind of problem, an intense research activity was begun after the Millennium Bridge in London was closed

*Corresponding author. Tel.: +39 11 090 4870; fax: +39 11 090 4999.
E-mail address: luca.bruno@polito.it (L. Bruno).

0022-460X/$ - see front matter © 2008 Elsevier Ltd. All rights reserved.
doi:10.1016/j.jsv.2008.12.015

Nomenclature

a	coefficient for the expression of the pedestrian–pedestrian synchronisation
b	coefficient for the expression of the pedestrian–structure synchronisation
$\mathscr{C}$	damping operator
d_0	body depth of a motionless pedestrian
d_c	characteristic dimension of a cluster of pedestrians
d_s	sensory distance
F	lateral force exerted by pedestrians
F_{pp}	lateral force component due to the pedestrians synchronised to each other
F_{ps}	lateral force component due to the pedestrians synchronised to the structure
F_s	lateral force component due to the uncorrelated pedestrians
$\tilde{F}$	envelope of the lateral force exerted by pedestrians
$\tilde{F}_{pp}, \tilde{F}_{ps}, \tilde{F}_s$	envelope of the lateral force components
$\bar{F}_s$	amplitude of the lateral force exerted by a single pedestrian on a motionless deck
$\bar{F}_{\dot{\tilde{z}}}$	amplitude of the F_{ps} component in phase with lateral velocity of the deck
$\bar{F}_{\ddot{\tilde{z}}}$	amplitude of the F_{ps} component in phase with the lateral acceleration of the deck
f_{pl}	lateral step frequency
f_r	frequency ratio f_{pl}/f_s
f_s	structural natural frequency of interest
g	function that makes the walking velocity sensitive to the deck motion
i	time index
L	length of the footbridge span
$\mathscr{L}$	stiffness operator
m	mass of the crowd–structure system
m_c	crowd mass
m_s	structural mass
n	total number of pedestrians
n_{pp}	number of pedestrians synchronised to each other
n_{ps}	number of pedestrians synchronised to the structure
n_s	number of uncorrelated pedestrians
q	structural displacement
S_{pp}	coefficient of synchronisation among pedestrians
S_{ps}	coefficient of pedestrian–structure synchronisation
t	time
t_s	time at which pedestrians stop because of excessive deck vibrations
v	pedestrian velocity
v_M	mean maximum velocity
X	space coordinate along the footbridge length
Y	vertical space coordinate
$\tilde{\dot{z}}, \tilde{\ddot{z}}$	envelope of the deck lateral velocity and acceleration
$\dot{z}_c, \ddot{z}_c$	thresholds of motion perception
$\dot{z}_M, \ddot{z}_M$	maximum values of the lateral velocity and acceleration of the deck
$\dot{z}_s, \ddot{z}_s$	serviceability limits on the lateral velocity and acceleration of the deck
Z	lateral space coordinate
δ	space dislocation in the crowd density–-velocity relation
Δt	time step
Δt_r	stop-and-go time interval
$\Delta\tau$	synchronisation time delay
ΔX_c	space grid size in the crowd subdomain
ε	half-amplitude of the lock-in triggering region
γ	travel purpose parameter in the crowd density–velocity relation
η	function that describes the deck acceleration effect on S_{ps}
ρ	crowd density
ρ_c	critical density, upper limit for unconstrained free walking
ρ_{ca}	capacity density
ρ_h	maximum density during the crowd event
ρ_M	maximum admissible density
ρ_{sync}	crowd density corresponding to complete pedestrian synchronisation
Φ	shape of the first lateral mode of the deck

because of excessive lateral vibration. The results of these studies, which are reviewed in Ref. [3], represent the scientific background of some recently published design guidelines [4,5].

The most relevant data concerning pedestrian behaviour have been obtained using an empirical approach. Laboratory tests involving a pedestrian walking on both a motionless platform [6] and a laterally moving treadmill [2,7], as well as tests performed on actual footbridges [8], have been carried out to measure the lateral

force exerted by one pedestrian and interesting information about the synchronisation between the pedestrian and the structure has been obtained. Moreover, the behaviour of a pedestrian in a crowd has been investigated by means of in situ experiments [2] and through the observation of videos recorded during crowd events [1,2].

Several semi-empirical load models have been developed on the basis of the aforementioned experimental data, e.g. in Refs. [4,9,10]. Generally, the pedestrians are considered as a load that has to be applied to the structural dynamic system. To the authors' knowledge, the crowd was first modelled as part of a complex dynamical system in Refs. [11,12], where the modelling framework was presented. This framework is based on the decomposition of the coupled multiphysical crowd–structure dynamical system into two subsystems, the crowd and the structure, which interact with each other through forcing terms. The resulting, very simple model is capable of taking into account for some key features of the phenomenon, such as the self-limited nature of the structural vibration and the effects of various pedestrian traffic conditions [12]. The authors devoted their subsequent work to the development of each single model component. The effects of the structure vibrations on the crowd behaviour have been modelled in Ref. [13], where a relation between the crowd density, the walking velocity and the deck motion has been derived. The crowd-to-structure action has been developed in Ref. [14] using a new lateral force model, referring to pedestrian clusters, which is able to describe both pedestrian-to-pedestrian and pedestrian-to-structure synchronisation effects in each cluster.

In the present work, the updated components have been collected in the initial modelling framework. The improved model has been implemented in an ad hoc developed multiphysics numerical code. The model has been applied to an actual crowd event on a real footbridge, the T-bridge (Japan). Detailed in situ measurements of both the crowd conditions and structural response [1] allow a complete comparison with the computational results. The coupled system sensitivity to both structural and pedestrian design parameters has been evaluated through three parametrical studies.

The paper is developed in six more sections. Section 2 briefly recalls the proposed model and describes its upgraded components. Section 3 is devoted to the computational approach. The model is applied to a case study, the T-bridge in Japan, which is described in Section 4. In Section 5 the model is validated by simulating a real event occurred on the T-bridge. Sensitivity studies on the pedestrian biometrics and travel purposes, the incoming crowd density and the structural properties are then performed in Section 6. The concluding remarks are outlined in Section 7.

2. Mathematical model

The main features of the developed time domain model concern the mathematical and numerical partitioning of the coupled system into two physical subsystems and the two-way interaction between them, according to the so-called partitioned approach which was first proposed by Park and Felippa [15] and which is generally applied to fluid–structure interaction problems. In the following, each part of the model is briefly described, referring to the framework schematized in Fig. 1.

The partitioned approach allows the structure (S) and crowd (C) subsystems to be described by means of models with different dimensions even though, in the present work, they share the same global Cartesian spatial reference system: the footbridge deck spans along the X-axis, the Y-axis is the vertical axis and the Z-axis completes the right-handed oriented system.

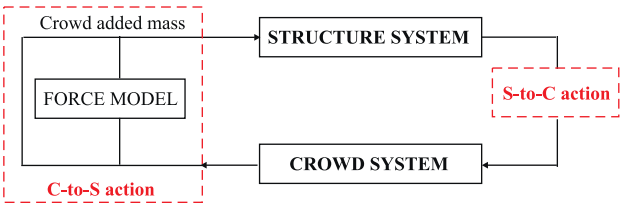

Fig. 1. Scheme of the time-domain coupled model.

2.1. The structure subsystem

The structure system is modelled as a nonlinear three dimensional (3D) damped dynamical system, whose equation of motion can be written as

$$[m_s + m_c(\rho)]\frac{\partial^2 q}{\partial t^2} + \mathscr{C}\left[\frac{\partial q}{\partial t}\right] + \mathscr{L}[q] = F(\rho, \ddot{\tilde{z}}), \tag{1}$$

where $q = q(X, Y, Z, t)$ is the structural displacement, X, Y, Z and t being the space and time independent variables; m_s and m_c are the structural and crowd mass, respectively; $\mathscr{C}$ and $\mathscr{L}$ are the damping and stiffness operators, respectively; $\rho = \rho(X, t)$ is the crowd density; F is the applied lateral force; $\ddot{\tilde{z}} = \ddot{\tilde{z}}(X, t)$ is the envelope of the lateral acceleration of the deck. Nonlinearity arises from two terms: first, the forcing term F is a function of both the crowd density and the lateral acceleration of the deck; second, the overall mass m is given by the sum of the structure and the crowd mass. The latter derives from the solution of the equation that governs the crowd subsystem, which in turn depends on the solution of the equation of motion of the structure (1).

2.2. The crowd subsystem

The crowd system is described by a one dimensional (1D) first-order macroscopic model [11,12], that is, the crowd is assumed to be a continuous fluid and its flow dynamics is described through the derivation of a mass conservation equation:

$$\frac{\partial \rho}{\partial t} + \frac{\partial}{\partial X}(\rho v) = 0, \tag{2}$$

where $v(X, t)$ is the crowd velocity. This equation obviously needs to be closed as two dependent variables (i.e. the crowd density and velocity) appear. A phenomenological relation which links the crowd velocity v to the crowd density is therefore introduced in the form proposed by the authors in Ref. [13]

$$v = v_M\left\{1 - \exp\left[-\gamma\left(\frac{1}{\rho} - \frac{1}{\rho_M}\right)\right]\right\}, \tag{3}$$

where v_M is the mean maximum velocity, ρ_M is the maximum admissible density and γ is a coefficient that makes the relation sensitive to different travel purposes (leisure/shopping, commuters/events, rush hour/business), which is obtained through a fitting of the data from Refs. [16,17]. Both v_M and ρ_M are made sensitive to the geographic area and the travel purpose by means of coefficients [13], which are determined from the observation data reported in Ref. [18]. In such a way, the model takes into account the biometrical and psychological factors that are known to affect crowd behaviour to a great extent.

A further improvement of the crowd model is proposed in this work by introducing a space dislocation into the crowd density–velocity relation, as first suggested in Ref. [19] in the theory of vehicular traffic flows:

$$v = v(\rho(X + \delta, t)), \tag{4}$$

where $\delta \geqslant 0$ is the anisotropic dislocation length. The crowd density ρ in the crowd density–velocity relation is therefore not a local density, but is forward dislocated in space. From the phenomenological point of view, the dislocation takes into account the pedestrians' attitude to react to what they see in a stretch of road in front of them. It is worth pointing out that the dislocation length is expected to depend on the walking speed, i.e. the faster the walking speed, the larger $\delta(v(\rho))$. In this sense, the dislocation length is analogous to the sensory distance d_s, which was defined by Fruin as the length required by a pedestrian to perceive, evaluate and react [17], except that the former is related to a cluster of pedestrians at the macroscopic scale, while the latter refers to one pedestrian at a microscopic scale. Bearing this analogy in mind, the dislocation length is defined as

$$\delta(\rho) = d_s(\rho)\frac{d_c}{d_0}, \tag{5}$$

where the $d_s(\rho)$ law was proposed by the authors in Ref. [13] by fitting experimental data [20], $d_0 = 0.36\,\mathrm{m}$ is the averaged body depth and d_c is the characteristic dimension of a cluster of pedestrians.

2.3. The structure-to-crowd action

In order to account for the structure-to-crowd action, the crowd density–velocity relation equation (3) has to be adapted to make the walking speed sensitive to the lateral motion of the deck. The following assumptions are retained from phenomenological observations:

- the motion of the platform, described by the envelope of its acceleration $\tilde{\ddot{z}}$, reduces the pedestrian walking velocity v;
- the pedestrians adjust their step to the platform motion with a synchronisation time delay $\Delta\tau$, which is expected to be greater than the time interval between two succeeding footfalls;
- after the pedestrians have stopped at time t_s because of excessive lateral vibrations, a stop-and-go time interval Δt_r elapses before they start walking again.

According to these hypotheses, the term v_M in the crowd density–velocity relation equation (3) is multiplied by a corrective factor $g(\tilde{\ddot{z}})$, which takes into account the sensitivity of v to the platform acceleration and has the trend:

$$g(\tilde{\ddot{z}}) = \begin{cases} 1 & \tilde{\ddot{z}} \leqslant \ddot{z}_c \cap t \geqslant t_s + \Delta t_r, \\ (\ddot{z}_M - \tilde{\ddot{z}}(X, t-\Delta\tau))/(\ddot{z}_M - \ddot{z}_c) & \ddot{z}_c < \tilde{\ddot{z}} < \ddot{z}_M \cap t \geqslant t_s + \Delta t_r, \\ 0 & \tilde{\ddot{z}} \geqslant \ddot{z}_M \cap t_s < t < t_s + \Delta t_r, \end{cases} \tag{6}$$

where $\ddot{z}_c \cong 0.2\,\mathrm{m/s^2}$ [21] corresponds to the threshold of motion perception, while $\ddot{z}_M = 2.1\,\mathrm{m/s^2}$ [8] is the maximum acceptable acceleration above which pedestrians stop walking.

2.4. The crowd-to-structure action

The crowd-to-structure action takes place in two ways. First, the mass m is constantly updated by adding the pedestrian mass m_c to the structural mass m_s. Second, the lateral force $F(t)$, exerted by the pedestrians, is expressed as a function of both the crowd density ρ and the envelope of the lateral acceleration of the deck $\tilde{\ddot{z}}$. A complete description of the macroscopic force model can be found in Ref. [14]: only a few basic points are given here. The lateral force F, exerted by a cluster of n pedestrians walking along a portion of the bridge span, is given by the sum of three terms:

$$F = F_{ps} + F_{pp} + F_s, \tag{7}$$

where F_{ps} is the force exerted by n_{ps} pedestrians synchronised with the structure, F_{pp} is the term due to n_{pp} pedestrians synchronised to each other and F_s is due to n_s uncorrelated pedestrians. The abovementioned numbers of pedestrians are defined as

$$\begin{aligned} n_{ps} &= nS_{ps}, \\ n_{pp} &= nS_{pp}(1 - S_{ps}), \\ n_s &= n - n_{ps} - n_{pp} \end{aligned} \tag{8}$$

by introducing two synchronisation coefficients S_{ps} and S_{pp}. The pedestrian–structure synchronisation coefficient S_{ps} is expressed as a function of the lateral acceleration of the deck $\tilde{\ddot{z}}$, by interpolating the data of Dallard et al. [2], and of the ratio $f_r = f_{pl}/f_s$:

$$S_{ps}(\tilde{\ddot{z}}, f_r) = [1 - \mathrm{e}^{-b(\tilde{\ddot{z}} - \ddot{z}_c)}][\mathrm{e}^{[-\eta(f_r - 1)^2]}], \tag{9}$$

where $\eta(\tilde{\dot{z}}) = 50e^{(-20\tilde{\dot{z}}/\pi)}$ and $b = 2.68$. The pedestrian–pedestrian synchronisation coefficient S_{pp} is calculated as a function of the crowd density ρ:

$$S_{pp} = \frac{1}{2}\left\{1 + \mathrm{erf}\left[a\left(\rho - \frac{\rho_{\mathrm{sync}} + \rho_c}{2}\right)\right]\right\}, \tag{10}$$

where $a = 3.14$, $\rho_c = 0.3\,\mathrm{ped/m^2}$ is the upper limit for unconstrained free walking and $\rho_{\mathrm{sync}} = 1.8\,\mathrm{ped/m^2}$ is the density value that corresponds to the total synchronisation of the pedestrians.

The component F_{ps} is expressed as

$$F_{ps} = n_{ps}[\bar{F}_{\tilde{\ddot{z}}}\sin(2\pi f_s t) + \bar{F}_{\tilde{\dot{z}}}\cos(2\pi f_s t)], \tag{11}$$

where $\tilde{\dot{z}}$ is the envelope of the lateral velocity time history of the deck, $\bar{F}_{\tilde{\ddot{z}}}$ and $\bar{F}_{\tilde{\dot{z}}}$ are the amplitudes of the components in phase with the lateral acceleration and velocity of the deck, respectively, which were obtained from Pizzimenti's data [7] (Fig. 2) and f_s is the frequency of the excited lateral structural mode. The latter is selected as the mode whose frequency falls in the pedestrian–structure synchronisation range, which is assumed to be [0.5 1.2] Hz, and which gives the highest contribution to the structural response.

The component F_{pp} is expressed as

$$F_{pp} = n_{pp}\bar{F}_s \sin(2\pi f_{pl} t), \tag{12}$$

where $\bar{F}_s \approx 30\,\mathrm{N}$ is the medium amplitude of the lateral force exerted by one pedestrian on a motionless deck and f_{pl} is the pedestrian lateral walking frequency, which is calculated as a function of the walking velocity v [14], using the experimental data of Bertram and Ruina [22]:

$$f_{pl} = (0.35v^3 - 1.59v^2 + 2.93v)/2. \tag{13}$$

Finally, the component F_s is expressed as

$$F_s = \sqrt{n_s}\bar{F}_s \sin(2\pi f_{pl} t), \tag{14}$$

according to the model proposed by Matsumoto and coworkers [23].

3. Computational approach

The mathematical model is solved by means of computational simulations performed in the space and time domains. The coupled system is decomposed by differential partitioning, that is, the system is first decomposed into subsystems (or fields) and then each field is spatially discretised separately [15]. The differential partitioning allows each field to be treated with discretisation techniques and solution algorithms that are known to perform well for the isolated system and it also allows non-matching grids to be used.

The 1D crowd field is discretised in space using the finite difference method. The nonlinear mass conservation partial differential equation is approximated through the Lax–Friederichs scheme, in its conservation form, to guarantee convergence to the solution [24]. The time derivative is replaced by a forward-in-time approximation, which means that the solution at time $i+1$ only depends on the solution at the

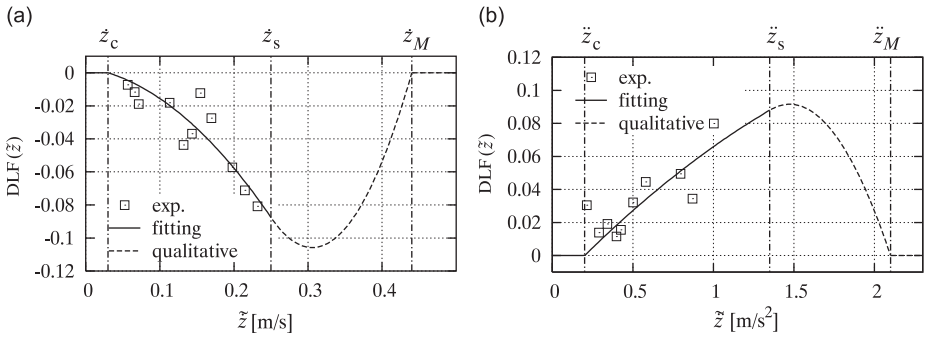

Fig. 2. Dynamic load factors (*DLF*s) referring to the F_{ps} components.

previous time i (first-order explicit scheme). The finite element method is employed for the space discretisation of the 3D structural multidegree-of-freedom (mdof) model, while its advancement in time is obtained by means of the Newmark method [25].

The two subsystems are characterised by non-matching grids in space, while they share the same discretisation in time. The structure space grid is coarser than the crowd grid, since the structure deformed shape requires fewer nodes to described it than the pedestrian traffic phenomena, because the first global lateral modes of the deck are expected to be mainly excited. A uniform space grid is adopted for the crowd field discretisation: its cell size ΔX_c is assumed to be twice the body depth d_0 of a motionless pedestrian [13], in order to satisfy the continuity assumption of the model. The structure grid is not uniformly spaced and contains classical 2-node beams and trusses with 6 and 3 dofs per node, respectively. Conservative interpolation [26] between the crowd and the structural grids, referring to the bridge deck, is adopted to numerically evaluate the crowd added mass, while distributed quantities (e.g. ρ) are interpolated with a standard quadratic interpolation. The adopted dimensionless time step is $\Delta t^* = \Delta t \cdot v_M/L = 1.7\text{e}-4$. The computational simulations are performed on the dimensionless form of the overall model, which means that all the variables are scaled with respect to reference quantities [12], that is, ρ_M, v_M and the overall bridge span length L. In the following, reference is made to the variable dimensional values in order to understand their physical meaning more clearly.

4. Description of the case study: the T-bridge

The proposed model has been tested by simulating a crowd event on the T-bridge (Toda Park Bridge, Toda City, Japan). The T-bridge was chosen since it has been extensively described by Fujino and coworkers in several papers [1,8,9,27] and particular attention has been devoted to the description of both the crowd conditions and the structure response during the events, in order to allow a detailed comparison between the experimental measurements and the simulated response. In the following, only some characteristics are mentioned.

The T-bridge is a cable-stayed footbridge with a two-span continuous steel box girder, a two-plane multistay cable system with 11 stays per plane and a 61.4 m-high tower made of reinforced concrete. The total bridge length L is about 180 m and the road deck width is 5.25 m. The deck mass is 800 kg/m^2 and the damping ratio is around 0.7%. The tower and the deck are modelled with elastic beam elements, while each cable is modelled using a single truss element (Fig. 3). The damping is modelled via Rayleigh stiffness proportional damping [28].

Fujino et al. [1] observed that some cables vibrated with a frequency close to 1 Hz during crowd events. The inertial contribution of the vibrating cables has been taken into account in the model by adding an estimated

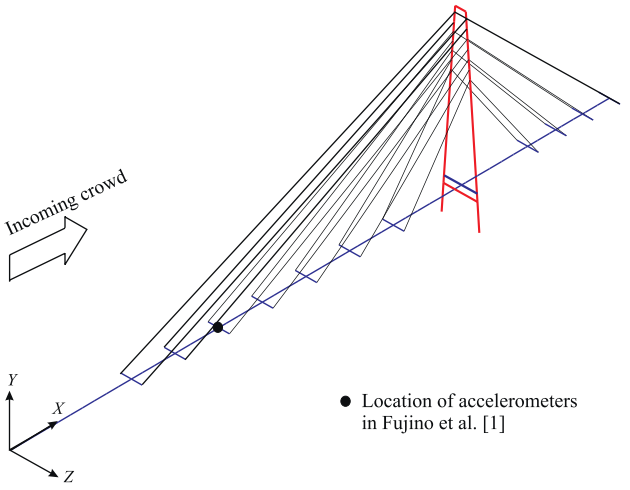

Fig. 3. The FE model of the T-bridge.

equivalent modal mass to the deck nodes that provide cable anchorages, as suggested by Fujino et al. [1]; the nonlinear behaviour of the cable has been taken into account by introducing the effective axial modulus of elasticity [29].

The modal properties provided by the FE model have been compared with footbridge natural frequencies and mode shapes reported by Fujino et al. [1] (Fig. 4).

It is worth pointing out that only the first lateral frequency falls in the pedestrian–structure synchronisation range, that is, [0.5 1.2] Hz (Eq. (11)). It can be observed that the first lateral frequency obtained using the FE model is higher (0.97 Hz) than the one obtained by Fujino et al. (0.9 Hz). Nevertheless, it should be noticed that the dominant frequency of the girder vibration recorded on the T-bridge was about 1 Hz when loading was small [1], and it decreased to about 0.93 Hz when the deck was congested and the vibration amplitude reached its maximum value [27]. Therefore, the obtained lateral frequency agrees with the deck behaviour in a non-congested crowd condition, while the added pedestrian mass is explicitly obtained from the solution of the mass conservation equation (2).

The footbridge connects a boat race stadium to a bus terminal. Therefore, at the end of boat races, the bridge is crossed by a great number of pedestrians who leave the stadium to reach the bus terminal. The different crowd conditions recorded on the T-bridge have been described in a qualitative way in several papers. The most crowded event is reported in Ref. [1], when more than 20 000 people left the stadium and crossed the bridge in about 20 minutes. In the most congested situation, about 2000 people walked simultaneously on the bridge. Less crowded situations are described in other papers [8,9,27]: a maximum number of around 12 000 people crossed the bridge in 12–20 minutes, with a crowd density varying between 0.8 and 1.5 ped/m^2. The simulated condition represents an average of the events reported in literature. The initial condition on the density is $\rho(X,0) = 0.01\,\mathrm{ped/m^2}$, while the boundary condition (bc) at the inlet $\rho(0,t)$ (Fig. 5a) has been set to allow about 14 000 pedestrians to pass over the bridge in 23 minutes, with a maximum density of $\rho_h = 1.33\,\mathrm{ped/m^2}$.

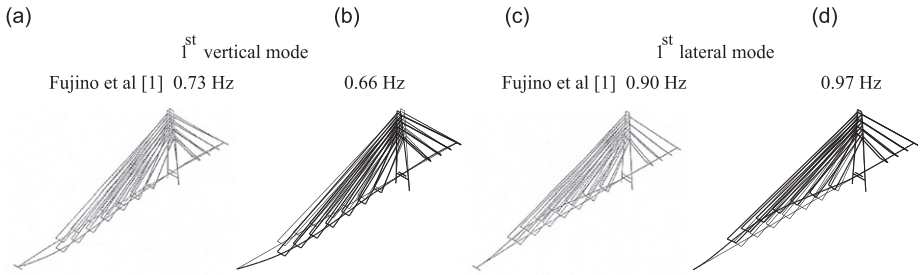

Fig. 4. Comparison between the frequencies reported by Fujino et al. [1] (a and c) and the ones obtained with the actual model (b and d).

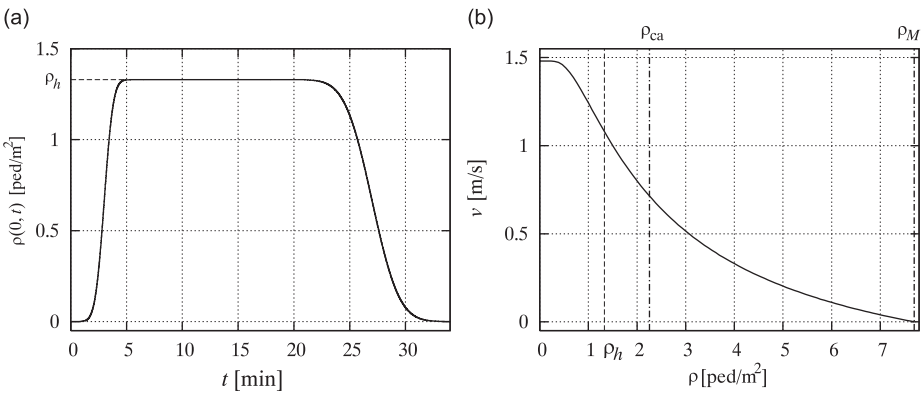

Fig. 5. Inlet bc on the crowd density (a) and velocity–density relation (b).

The incoming density shows a steady-state regime bounded between two transient ones, which correspond to the start and the end of the stadium evacuation. It should be noticed that the density decreases in a smoother way than the initial increase. This is due to the assumption that the stadium evacuation abruptly starts at the end of the boat race with a sudden increase in the crowd density, while the complete evacuation is expected to be smoother in time. The velocity–density relation has been adapted for the case of Asia and rush-hour traffic, that is, $\rho_M = 7.7\,\mathrm{ped/m^2}$, $v_M = 1.48\,\mathrm{m/s}$ and $\gamma = 0.273\rho_M$ [13] (Fig. 5b). The maximum density at inlet ρ_h does not exceed the capacity density ρ_{ca}, which corresponds to the maximum flow and to the lower bound of the congested regime.

5. Simulation of an actual event

The proposed approach allows the evolution of both subsystems to be described in space and time. Fig. 6 reports the time–space distributions of some of the main variables obtained from the computational simulation: the crowd density ρ, the envelope of the lateral acceleration of the deck $\tilde{\ddot{z}}$ and of the force components, expressed in (N/m). It is worth recalling that in the model $\tilde{\ddot{z}}$ is delayed in time by a quantity $\Delta\tau$, according to Eq. (6).

Five crowd regimes can be identified from the time–space distribution of the crowd density (Fig. 6a).

- Regime I 'advancing front': the leading pedestrians advance on the bridge, which is still partially empty.
- Regime II 'filling gradient': the crowd is in the transient condition of gradually filling the deck span.
- Regime III 'uniform crowd': the pedestrian density reaches its maximum value and is almost uniformly distributed along the footbridge.
- Regime IV 'vacating gradient': the crowd density gradually decreases at the footbridge entrance, but the whole span remains crowded.
- Regime V 'leaving front': the end of the crowd is leaving the footbridge, which is already partially empty.

The upper bound of regime I and the lower bound of regime V correspond to the maximum and minimum differences between the crowd density at the outlet and at the inlet $\Delta\rho = \rho(L,t) - \rho(0,t)$, respectively. Regime III is defined as the time window during which the averaged value of ρ along the span is equal to 99% of the maximum density ρ_h and the standard deviation is less than $0.01\rho_h$. The overall evolution in time of ρ is mainly due to the bc which is imposed at the inlet. In other words, the crowd dynamics is not affected by nonlinear traffic phenomena due to a crowd density above the capacity value ρ_{ca} or to the effects of excessive lateral acceleration of the deck, that is, $\tilde{\ddot{z}} \geqslant \ddot{z}_M$.

The previously defined regimes can also be recognised in the time behaviour of the other variables. It can, in fact, be noticed that the uniform crowd regime also corresponds to the highest values of the deck response ($\tilde{\ddot{z}} > \ddot{z}_c$, Fig. 6b), which reaches the steady-state condition in the same period of time. Regimes I and V are characterised by two local maxima of the structural response, which can be related to the well-known travelling load effects: the $\tilde{\ddot{z}}$ local maximum in regime I is mainly due to the F_s component, whose distribution excites the structural first mode, while the F_{pp} component is negligible, since the crowd density is below ρ_c in a large portion of the footbridge span; a similar, but specular, situation occurs in regime V. Not only the first lateral mode is excited: in the time interval 27–29 minutes, i.e. across regimes IV and V, the second lateral mode gives the most relevant contribution to the deck response, as shown in Fig. 6b.

During regime III, crowd–structure synchronisation takes place in the points where $\tilde{\ddot{z}}$ exceeds the threshold of motion perception $\ddot{z}_c$, therefore F_{ps} is not null and shows a space distribution that locally matches the deck deformed shape (Fig. 6c). The values of $\tilde{\ddot{z}}$, which are slightly higher than $\ddot{z}_c$ in the case-study, involve small values of the F_{ps} amplitude per synchronised-to-structure pedestrian ($|F_{ps}| \approx 5\,\mathrm{N/ped}$), although a non-negligible number of the pedestrians are synchronised with the deck ($n_{ps} \approx 20\%n$). As a consequence, the corresponding number of pedestrians synchronised to each other decreases, causing a decay of $|F_{pp}|$ (Fig. 6d). The walking frequency during regime III is equal to $f_{pl} = 0.87\,\mathrm{Hz}$, which is close to the natural lateral frequency ($f_s = 0.93\,\mathrm{Hz}$), therefore the frequency ratio $f_r = 0.935$ involves almost resonant conditions even for those pedestrians who are not perfectly synchronised with the structure. In the other regimes, when $\tilde{\ddot{z}} \leqslant \ddot{z}_c$, F_{pp} follows the same trend as ρ. F_s follows from the other two components: it has a relevant magnitude when

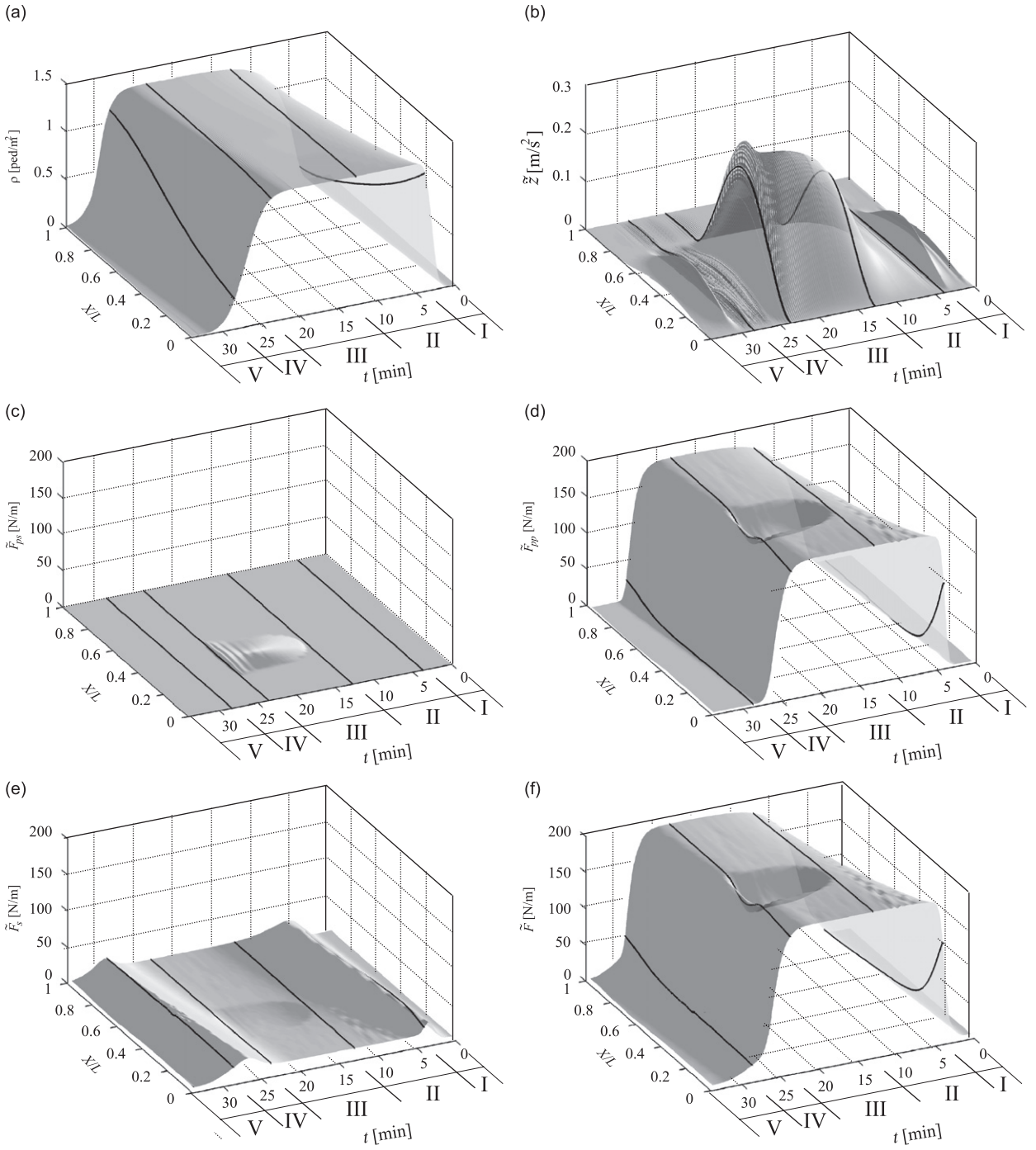

Fig. 6. Space–time distributions of the main variables.

both kinds of synchronisation are still not fully developed (across regimes I and II) or when they are vanishing (across regimes IV and V), that is, if $\rho \leqslant \rho_c$ and $\tilde{\ddot{z}} \leqslant \ddot{z}_c$ (Fig. 6e). Fig. 6f clearly shows that the resulting total force F is mainly due to the F_{pp} component (in regime III, $|F| = 28.8\,\mathrm{N/ped}$, $|F_{pp}| \approx 27\,\mathrm{N/ped}$).

Finally, the results of the computational simulation are compared to the measurements reported in Ref. [1] for five time windows (Fig. 7). The time windows reported by Fujino and co-workers do not exactly match the aforementioned five regimes, but were probably defined with a similar objective, that is, to qualitatively

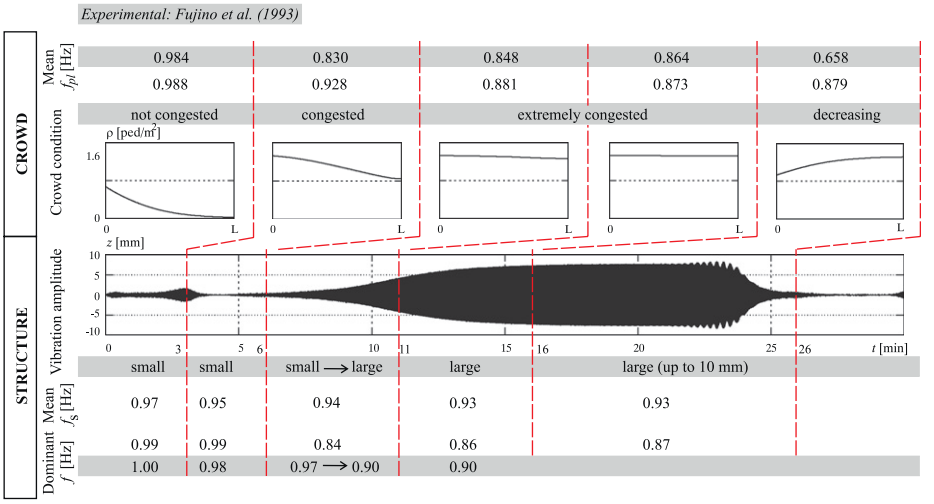

Fig. 7. Comparison between the simulated results and the data reported in Ref. [1].

identify the different crowd conditions that occurred during the event. As for the structure results, the figure reports: the time history of the lateral displacement of the deck in the node corresponding to the position of the installed accelerometers [1] (Fig. 3); the first lateral frequency f_s, obtained through modal analysis at each time step and averaged over the time window; the dominant frequency f, obtained through the displacement power spectral density in the same window. The instantaneous spatial distributions of the crowd density at the end of each time window are also reported in Fig. 7 as far as the crowd results are concerned, together with the mean walking frequency f_{pl} averaged over the time window.

Looking at the results, a very good agreement is evident between the simulation and the recorded data. The maximum amplitude of the lateral deck displacement, which is about 9 mm, matches the measured data very well. The maximum percentage of pedestrians synchronised with the structure ($n_{ps}/n = 21\%$) is also in very good agreement with that estimated from the observation ($n_{ps}/n \approx 20\%$, [1]). Similar considerations can be made for all the considered variables. The dominant frequency of the deck vibration is always closer to the walking frequency than to the lateral frequency of the structure. This outcome confirms that the force components, due to pedestrians synchronised-to-each-other or uncorrelated, are dominant with respect to that due to pedestrians synchronised with the structure.

6. Sensitivity studies on design parameters

Three sensitivity studies have been performed on the same real structure in order to highlight how different design conditions (the travel purposes and the geographic area in which the bridge is built, the actual crowd density, the structural deck–tower constraints which can be realised) can dramatically affect the response of a real structure.

6.1. Sensitivity study on travel purposes and geographic areas

Four computational simulations have been performed with different crowd density–velocity relations in order to test the sensitivity of the structural response to different travel purposes or geographical areas. The velocity–density relation (Eq. (3)) was characterised each time by varying the coefficient γ and the value of ρ_M and v_M for the following combinations: Asia-rush hour (AR), Asia-commuters (AC), Asia-leisure (AL) and USA-leisure (UL), which correspond to a progressive decrease of v for $\rho > 0.8\,\mathrm{ped/m^2}$ (Fig. 8a). The first case (AR) refers to the condition that actually occurred on the T-bridge, which was previously simulated and commented in Section 5. The substitution of the four fundamental laws in Eq. (13) leads to the $f_{pl}-\rho$ relations shown in Fig. 8b.

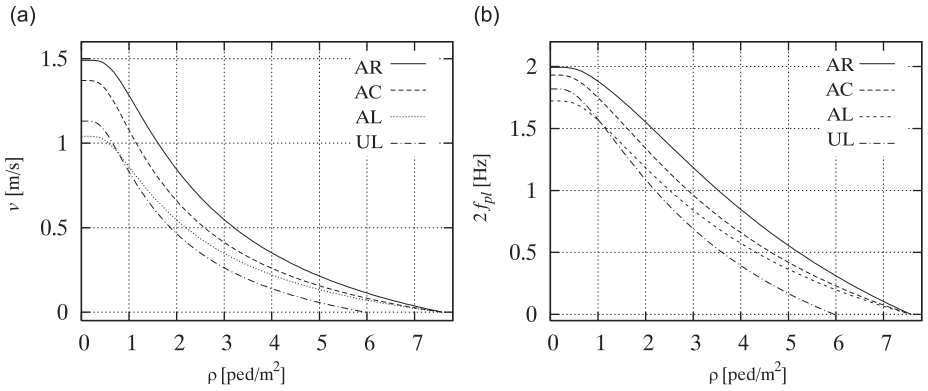

Fig. 8. $v(\rho)$ (a) and $f_{pl}(\rho)$ (b) relations.

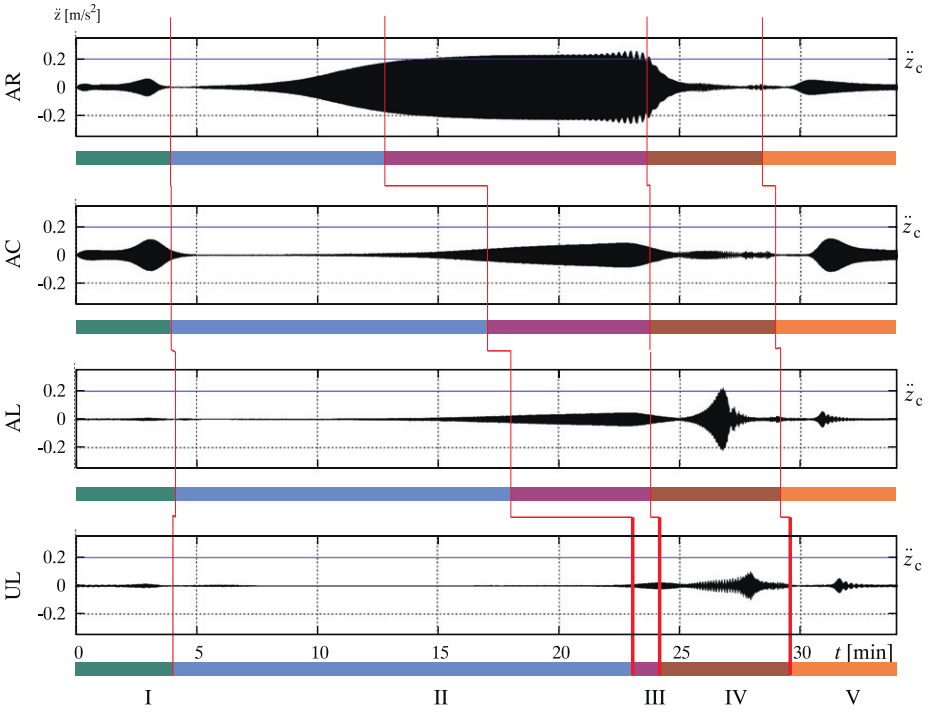

Fig. 9. Time histories of the lateral acceleration of the deck at $X/L = 0.3$.

The five regimes described above were identified for the four cases and outlined in Fig. 9, which plots the deck acceleration time histories at $X/L = 0.3$.

The dramatic differences in the structural response are due to the different kinds of traffic that were considered. In particular, the lower the pedestrian velocity (it monotonically decreases from AR to UL), the longer regimes I and II, i.e. the time required to cross the span and to fill the footbridge. Therefore, for a given incoming crowd bc, regime III, along which the maximum and uniform pedestrian load occurs, is monotonically delayed and shortened from 11 minutes in the AR case to 1 minute in the UL case. The related deck response is progressively shifted in time and in turn reduced in amplitude.

A deeper insight into the relations among the main variables is provided in Fig. 10, which shows the time–space evolution of the crowd density, deck lateral acceleration and frequency ratio for each case.

The four cases show similar distributions of ρ in regimes I and V. The deck response is once more due to the travelling load effects, but the different amplitudes of deck response can be explained by looking at the f_r

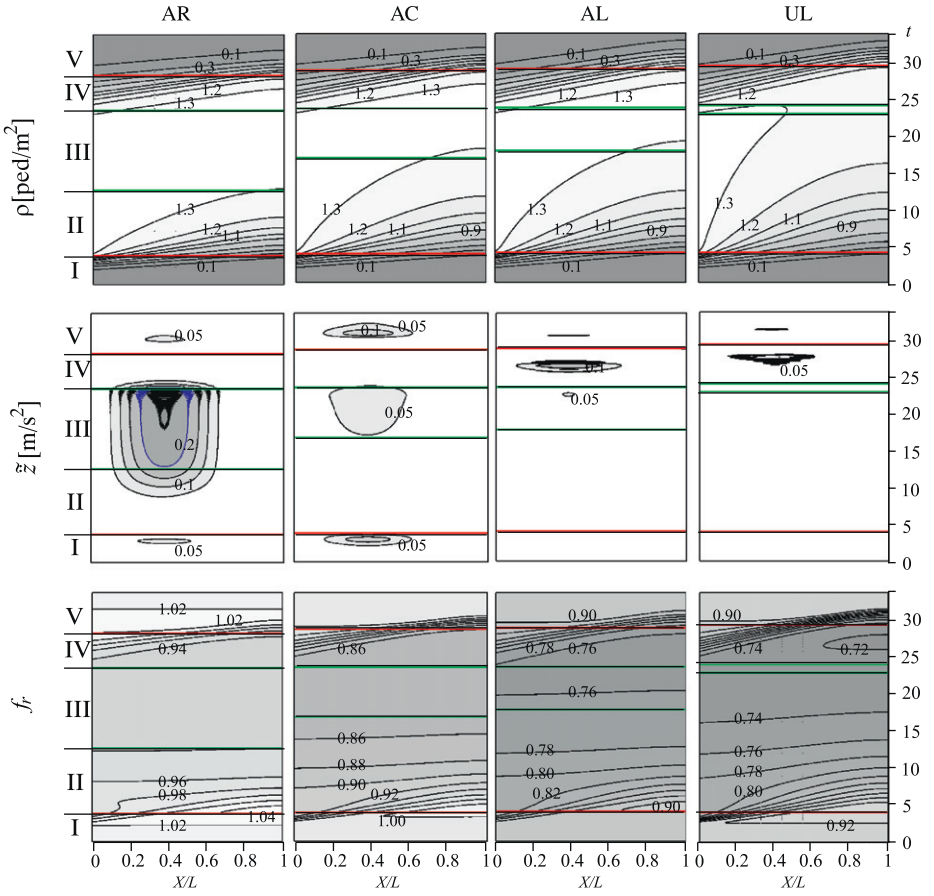

Fig. 10. Evolution in space and time of the main variables.

diagram (Fig. 10, third row): the highest amplitudes correspond to the value of f_r that is closest to unity (AC, $f_r = 1$; AR, $f_r = 1.02$), which means that the force is almost resonant with the first lateral mode of the deck. The uniform crowd condition observed during regime III reflects on f_r, which is almost constant along the span. Once more, the AR case is the closest to the resonant condition, therefore the acceleration amplitude only grows and exceeds the lock-in threshold $\ddot{z}_c$ in this case.

The sensitivity study on the crowd density–velocity relation shows that different crowd travel purposes can lead to quite different structural responses: for the case-study, the rush-hour traffic causes a deck vibration amplitude which is almost three times greater than the one obtained in leisure traffic conditions for the same geographical area. For this reason, footbridges should be designed according to the type of pedestrian traffic which is most likely to occur on the bridge during its lifetime, as already recommended in Ref. [4].

6.2. Sensitivity study on the crowd bcs

The second sensitivity study was performed on the crowd bcs at the inlet, by varying the maximum value reached by the density ρ_h (Fig. 11). It is worth recalling that the case $\rho_h = 1.33\,\mathrm{ped/m^2}$ corresponds to the actual event condition that was simulated in Section 5.

Fig. 12 shows the time histories of the lateral acceleration of the deck at $X/L = 0.3$.

First, it should be noticed that the maximum amplitude of the lateral acceleration of the deck does not correspond to the case with the highest density $\rho_h = 2\,\mathrm{ped/m^2}$. This can be easily explained by looking at the data in Table 1. Increasing values of ρ_h correspond to increasing amplitude of the total force, but also to a decrease in f_r due to the effect of the crowd added mass. As a consequence, when $\rho_h = 0.8\,\mathrm{ped/m^2}$, the total

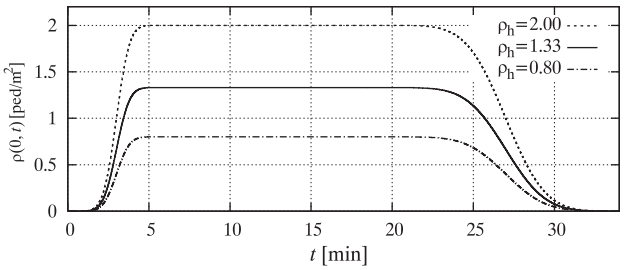

Fig. 11. Inlet bc of the density.

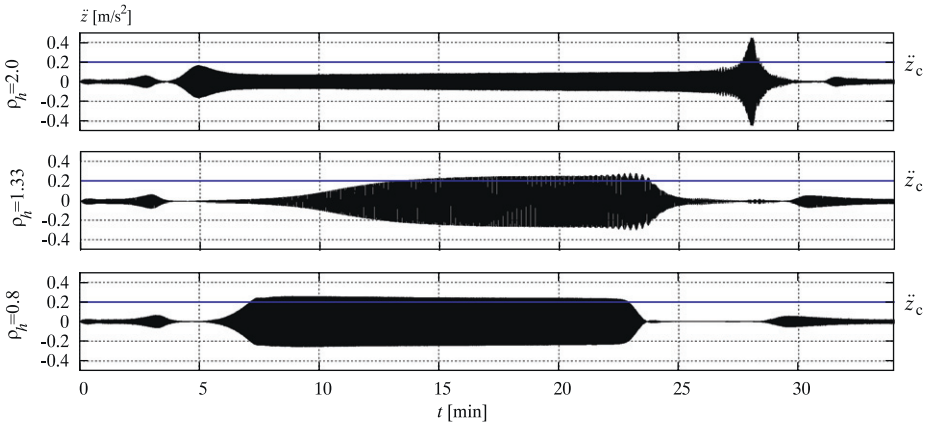

Fig. 12. Time histories of the lateral acceleration of the deck at $X/L = 0.3$.

Table 1
Mean values of the main variables during regime III.

ρ_h (ped/m^2)	2	1.3	0.8
f_r	0.85	0.93	1.01
$\|F\|$ (N)	1122	719	169
$\ddot{\bar{z}}_{\max}$ (m/s^2)	0.10	0.25	0.27

force magnitude is one order of magnitude lower that in the case of $\rho_h = 2\,\mathrm{ped/m^2}$, but the force is almost resonant with the first mode of the deck ($f_r = 1.01$) and it therefore induces the highest structural response.

Second, the almost steady-state response for $\rho_h = 2\,\mathrm{ped/m^2}$ is due to the fact that, in regime III, the crowd density exceeds the value $\rho_{\mathrm{sync}} = 1.8\,\mathrm{ped/m^2}$, above which $S_{pp} = 1$. Therefore, all pedestrians are synchronised to each other and walk with the same frequency, which is sufficiently far from f_s to prevent resonance ($f_r \approx 0.85$).

This study once more demonstrates the nonlinearity and complexity of the coupled system. For the analysed case-study, in fact, the lower structural response has been obtained for the highest value of crowd density. This is due to the effects of the crowd added mass, which changes the dynamical properties of the footbridge, and of the crowd density–velocity relation, which influences the lateral walking frequency: both phenomena affect the f_r ratio.

6.3. Sensitivity study on the structural stiffness

Finally, the influence of the dynamic properties of the structure on the coupled-system behaviour has been investigated. The aim of this study is to evaluate the effects that different amplitudes of the deck response have

on the synchronisation phenomena. This objective is obtained by varying the flexural stiffness of the deck in the horizontal plane. The change in the deck stiffness is obtained by changing the way in which the deck is constrained at the tower position rather than by varying its inertial properties, bearing in mind that the sensitivity analyses presented in this paper are not performed on an ideal benchmark, but on a real footbridge, and that the determination of the deck–tower constraint is a key issue in the design of cable-stayed bridges [30]. The constraint conditions are defined according to the scheme reported in Fig. 13:

- case A: the deck is not directly connected to the tower: an external constraint inhibits all the translations and the rotations around the Y- and X-axes;
- case B: the deck is fixed to the tower by means of two rigid links. This constraint condition models the actual condition of the T-bridge;
- case C: the deck is not directly connected to the tower: an external constraint inhibits all the translations and the rotation around the X-axis.

The three different constraint conditions do not induce significant changes in the mode shapes of the first lateral mode along the main span (Fig. 14), therefore the dynamic response is mainly affected by the change in the natural frequencies (case A 0.96 Hz, case B 0.93 Hz, case C 0.83 Hz).

It can be noticed, from the deck acceleration time histories in Fig. 15, that case A is qualitatively similar to case B. The higher structural stiffness and the frequency ratio farther from unit than in case A explain the lower amplitude of the lateral vibrations of the deck, which are always under the critical value $\ddot{z}_c$.

The structural response of case C is quite different from the other cases that have been analysed. Nevertheless, once again, it is possible to identify a correspondence between the crowd regimes and the structural response. Let us focus on the uniform crowd regime III, along which the deck acceleration shows a periodic evolution of $\tilde{\ddot{z}}$, with a characteristic time-scale of about 24 s. The time histories of the main variables at $X = 0.3L$, during one period, are plotted in Fig. 16. When $\tilde{\ddot{z}} > \ddot{z}_c$, the higher $\tilde{\ddot{z}}$, the lower the walking velocity v, because of the structure-to-crowd action modelled in Eq. (6). The crowd density in turn varies slightly, oscillating around a mean value that is higher than the maximum density at the inlet boundary ($\bar{\rho} = 1.35 > \rho_h = 1.33$): in other terms, the lateral oscillation of the deck involves a closer packing of the faster incoming pedestrians upstream from the maximum acceleration deck section ($X/L = 0.4$). The acceleration

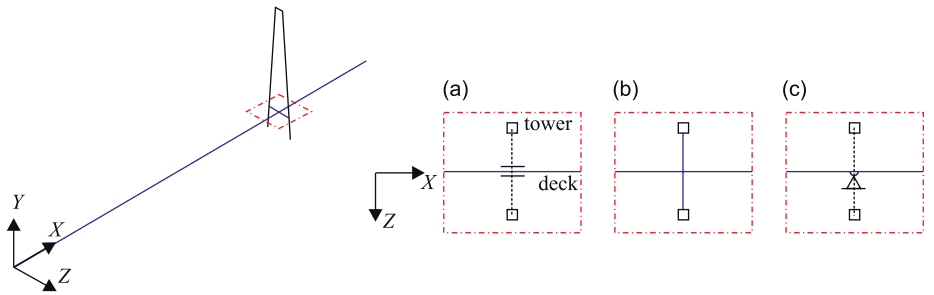

Fig. 13. Scheme of the deck–tower constraint conditions.

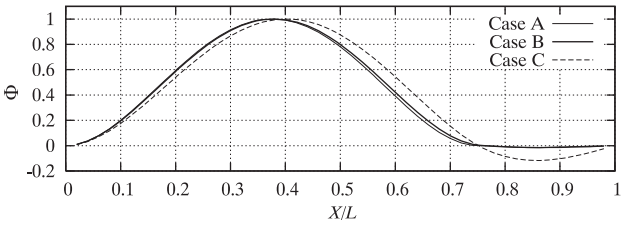

Fig. 14. Mode shapes of the first lateral mode.

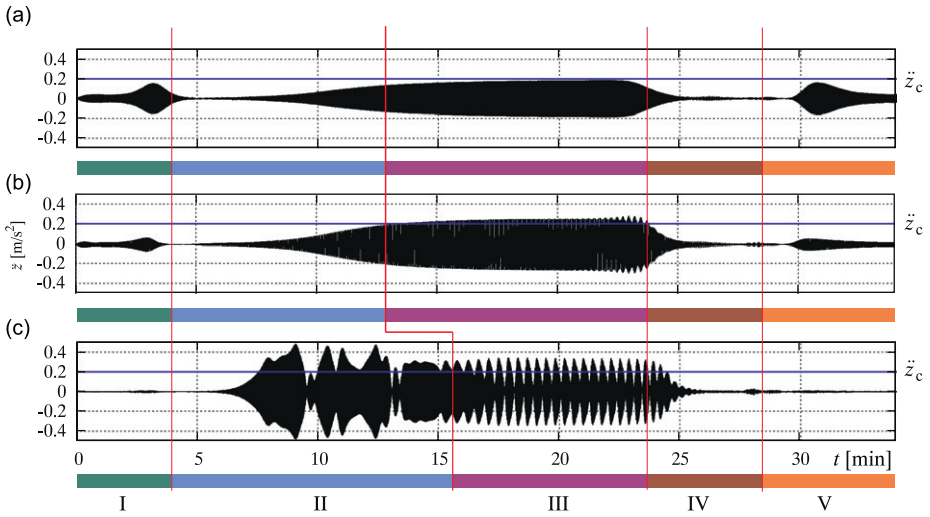

Fig. 15. Time histories of the lateral acceleration of the deck at $X/L = 0.3$.

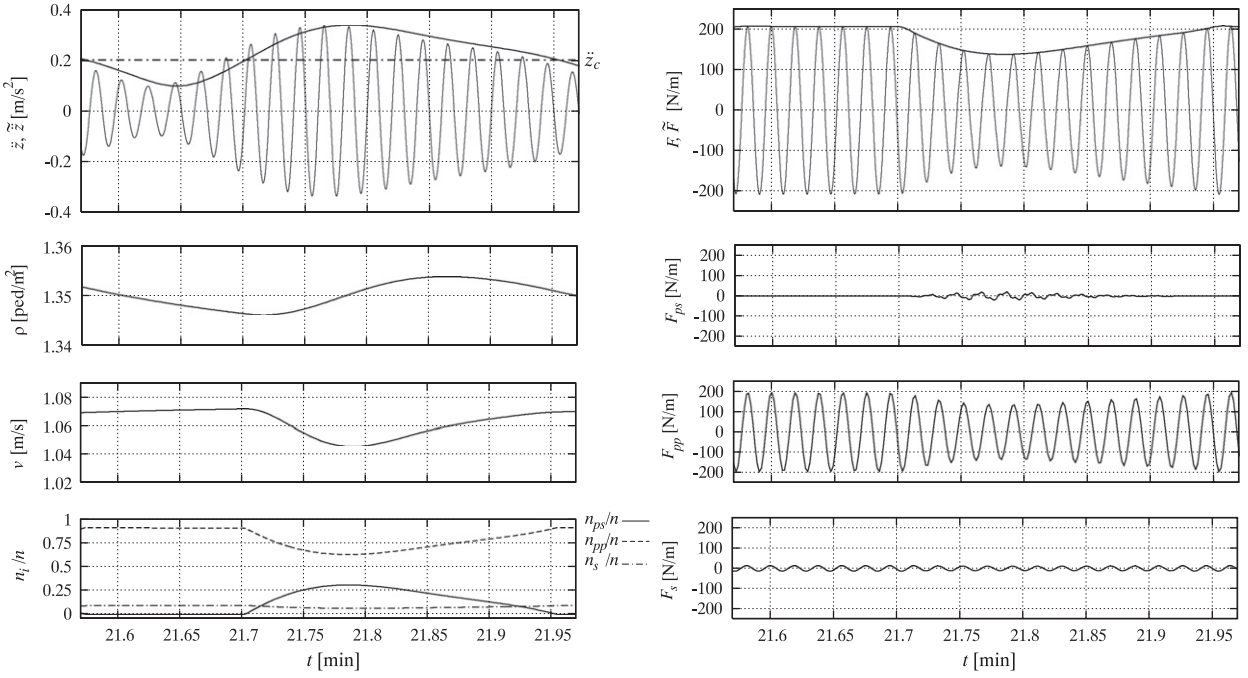

Fig. 16. Case C, regime III: time histories of the main variables at $X/L = 0.3$.

amplitude induces more relevant effects on the percentages of synchronised pedestrians: n_{ps} grows with $\tilde{\ddot{z}}$ when $\tilde{\ddot{z}} > \ddot{z}_c$ up to $n_{ps}/n \approx 30\%$, while it is null when the acceleration is below the critical value. The slight variation in the crowd density does not dramatically affect the percentage of pedestrians synchronised to each other, n_{pp}, but the latter is reduced by the same acceleration amplitude, in the sense that the pedestrians synchronised to the structure are subtracted from the pedestrians who are synchronised to each other. Hence, n_{pp} reaches its minimum ($n_{pp} \approx 60\%$) when n_{ps} reaches its maximum.

The total force F is mainly due to the F_{pp} component, as is clearly shown in the graphs in the second column of Fig. 16. This means that synchronisation among pedestrians plays a leading role in determining the crowd load, as already pointed out for the previous simulations. The amplitude of F_{ps} is, in fact, negligible with

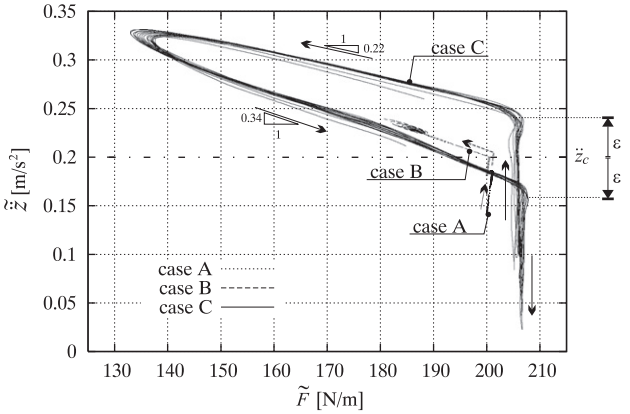

Fig. 17. Regime III: force–acceleration envelope diagrams at $X/L = 0.3$.

respect to F_{pp}, both because $n_{ps} < n_{pp}$ and because the *DLF*s corresponding to the reached deck acceleration and velocity are smaller than the *DLF* on a motionless platform (Fig. 2). The total force envelope $\tilde{F}$ therefore roughly follows the n_{pp} time history and shares the same dependency on the deck acceleration amplitude $\tilde{\ddot{z}}$. The maximum force amplitude corresponds to the time window during which the acceleration is below the critical value; the resulting growth of the acceleration amplitude in turn involves a decrease in the force amplitude, which is followed by a lateral oscillation decay. The inverse proportional relation between the force and the acceleration envelopes suggests a further self-limiting mechanism of the structural response, for the low acceleration amplitudes simulated in case C. This mechanism differs from the one explicitly taken into account in the model formulation, which occurs at a very high acceleration amplitude, at which pedestrians stop walking.

The $\tilde{\ddot{z}}$–$\tilde{F}$ diagram during regime III at $X/L = 0.3$ is plotted in Fig. 17 for the A–C cases. The arrows show the direction of the trajectories.

The following considerations can be made:

- in case A, the acceleration amplitude monotonically grows versus an almost constant force amplitude, even though the former never exceeds its critical value;
- in case B, the acceleration amplitude exceeds its critical value, and the further growth of $\tilde{\ddot{z}}$ involves the decay of the force amplitude. Once more, the evolution of $\tilde{\ddot{z}}$ is mainly monotonic, in the sense that an orbit-like diagram is only detected at the highest values of $\tilde{\ddot{z}}$, which are reached at the end of regime III (Fig. 15);
- in case C, a limit cycle in the $\tilde{\ddot{z}}$–$\tilde{F}$ plane is reached during the whole of regime III, coherently with what has been discussed above:
  - the lock-in effects do not take place at $\tilde{\ddot{z}} = \ddot{z}_c$, but are postponed by a quantity ε, i.e. the self-limited response occurs at $\ddot{z}_c + \varepsilon$, if the system enters the lock-in stage (growing $\tilde{\ddot{z}}$) and at $\ddot{z}_c - \varepsilon$, if the system exits from the lock-in stage (decaying $\tilde{\ddot{z}}$). The $\ddot{z}_c \pm \varepsilon$ range can be regarded as a triggering threshold region instead of a point-wise triggering condition. Its amplitude 2ε is supposed to depend on the acceleration amplitude oscillation during the limit cycle;
  - two almost linear parts of the limit cycle, which are characterised by rather different slopes, can be easily observed. In more physical terms, the acceleration decays faster than it grows, i.e. the system exits from the lock-in stage more quickly than it enters.

7. Concluding remarks

A complete model has been proposed to simulate the phenomenon of synchronous lateral excitation on lively footbridges. The model is based on the partitioning of the coupled system into two interacting subsystems. The crowd is not intended as just a load, but as a part of a complex dynamical system.

The model was first applied to simulate a real event that occurred on the T-bridge in Japan, and then subjected to several sensitivity studies on different crowd and structural parameters. The results obtained from the simulation of a real event show an excellent agreement with the recorded data, both for the evolution in time of the crowd condition along the span and for the maximum value of the lateral displacement of the deck.

Generally speaking, the sensitivity studies highlight the capabilities of the proposed approach to evaluate the effects of various physical parameters on the crowd dynamics and structural response.

The structural response is particularly sensitive to the crowd travel purpose and geographical area. Hence, in the conceptual design phase, it is important to plan the kind of pedestrian traffic that the footbridge is most likely to incur during its lifetime.

The sensitivity study on the crowd density has shown that a more crowded condition does not always correspond to higher deck vibrations and confirmed the complexity of the coupled dynamical system. This conclusion has obviously been derived from the assumptions that were made for the proposed model. Simplified comfort criteria, based on the limitation of the number of pedestrians crossing the bridge, might not always be effective in preventing the synchronous lateral excitation phenomenon. However, the complexity of the phenomenon makes it difficult to conceive compact comfort criteria which can take into account all the features involved.

Finally, the sensitivity study on the structural stiffness has allowed the most relevant effects of deck acceleration to be considered in the neighbourhood of the acceleration critical value. A limit cycle in the force–acceleration envelope plane can be observed. This shows a self-limiting mechanism of the structural response around the lock-in triggering threshold region, which gives rise to intermittent lock–delock stages. These simulated features strengthen the analogy with the lock-in phenomenon that occurs in fluid–structure interaction and which has been suggested in literature. A structural benchmark, characterised by lower lateral stiffness, could provide more information on the effects of very high amplitudes of deck acceleration on crowd–structure interaction.

Acknowledgements

The authors wish to thank Y. Fujino and S. Nakamura for kindly providing the structural properties of the T-bridge. This research has been carried on with the financial support of IABSE Foundation, of the Lagrange Project—ISI Foundation and of the Italian Ministry of Education, University and Research M.I.U.R. within the project Aeroelastic phenomena and other dynamic interaction on non-conventional bridges and footbridges.

References

[1] Y. Fujino, B.M. Pacheco, S. Nakamura, P. Warnitchai, Synchronization of human walking observed during lateral vibration of a congested pedestrian bridge, *Earthquake Engineering and Structural Dynamics* 22 (1993) 741–758.

[2] P. Dallard, T. Fitzpatrick, A. Flint, S.L. Bourva, A. Low, R.M. Ridsdill, M. Willford, The London Millennium footbridge, *The Structural Engineer* 79 (22) (2001) 17–33.

[3] S. Živanović, A. Pavic, P. Reynolds, Vibration serviceability of footbridges under human-induced excitation: a literature review, *Journal of Sound and Vibration* 279 (2005) 1–74.

[4] Fédération Internationale du Béton, Guidelines for the design of footbridges, fib Bullettin N.32, November 2005.

[5] Sétra/AFGC, Passerelles piétonnes. Évaluation du comportement vibratoire sous l'action des piétons, Mars 2006.

[6] T.P. Andriacchi, J.A. Ogle, J.O. Galante, Walking speed as a basis for normal and abnormal gait measurements, *Journal of Biomechanics* 10 (1997) 261–268.

[7] A.D. Pizzimenti, F. Ricciardelli, Experimental evaluation of the dynamic lateral loading of footbridges by walking pedestrians, 6*th International Conference on Structural Dynamics*, Paris, 2005.

[8] S. Nakamura, Field measurement of lateral vibration on a pedestrian suspension bridge, *The Structural Engineer* 81 (22) (2003) 22–26.

[9] S. Nakamura, T. Kawasaki, Lateral vibration of footbridges by synchronous walking, *Journal of Constructional Steel Research* 62 (2006) 1148–1160.

[10] G. Piccardo, F. Tubino, Parametric resonance of flexible footbridges under crowd-induced lateral excitation, *Journal of Sound and Vibration* 311 (2008) 353–371.

[11] F. Venuti, L. Bruno, N. Bellomo, Crowd–structure interaction: dynamics modelling and computational simulation, *Proceedings Footbridge* 2005, Venezia, 2005.

[12] F. Venuti, L. Bruno, N. Bellomo, Crowd dynamics on a moving platform: mathematical modelling and application to lively footbridges, *Mathematical and Computer Modelling* 45 (2007) 252–269.
[13] F. Venuti, L. Bruno, An interpretative model of the pedestrian fundamental relation, *Compte Rendu Mecanique* 335 (2007) 194–200.
[14] F. Venuti, L. Bruno, Pedestrian lateral action on lively footbridges: a new load model, *Structural Engineering International* 17(3).
[15] K.C. Park, C.A. Felippa, C. Farhat, Partitioned analysis of coupled mechanical systems, University of Colorado, Report No. CU-CAS-99-06, March 1999.
[16] D. Oeding, Verrkhersbelastung und Dimensionierung von Gehwegen und anderen Anlagen des Fußgangerverkhers, *Strassenbau and Strassenverkherstechnik* 22 (1963) 36–40.
[17] J.J. Fruin, *Pedestrian Planning and Design*, Elevator World Inc., 1987.
[18] S. Buchmueller, U. Weidmann, Parameters of pedestrians, pedestrian traffic and walking facilities, ETH Zürich, ivt Report No. 132, October 2006.
[19] N. Bellomo, V. Coscia, First order models and closure of mass conservation equations in the mathematical theory of vehicular traffic flow, *Compte Rendu Mecanique* 333 (2005) 843–851.
[20] A. Seyfried, B. Steffen, W. Klingsch, M. Boltes, The fundamental diagram of pedestrian movement revisited, *Journal of Statistical Mechanics* 10.
[21] International Standardization Organization, Bases for design of structures—serviceability of buildings against vibrations, iSO 10137, 1992.
[22] J.E. Bertram, A. Ruina, Multiple walking speed–frequency relations are predicted by constrained optimization, *Journal of Theoretical Biology* 209 (2001) 445–453.
[23] Y. Matsumoto, T. Nishioka, H. Shiojiri, K. Matsuzaki, Dynamic design of footbridges, *IABSE Proceedings*, Vol. P17/78, 1978, pp. 1–15.
[24] R.J. Leveque, *Numerical Methods for Conservation Laws*, Birkhauser, Zurich, 1992.
[25] N.M. Newmark, A method of computation for structural dynamics, *ASCE Journal of the Engineering Mechanics Division* 85 (EM3) (1959) 67–94.
[26] C. Farhat, M. Lesoinne, P. LeTallec, Load and motion transfer algorithms for fluid/structure interaction problems with non-matching discrete interfaces: momentum and energy conservation, optimal discretization and application to aeroelasticity, *Computer Methods in Applied Mechanics and Engineering* 157 (1998) 95–114.
[27] S. Nakamura, Y. Fujino, Lateral vibration on a pedestrian cable-stayed bridge, *Structural Engineering International* 12 (4) (2002) 295–300.
[28] R. Clough, J. Penzien, *Dynamics of Structures*, McGraw-Hill, New York, 1987.
[29] P. Warnitchai, Y. Fujino, T. Susumpow, A non-linear dynamic model for cables and its application to a cable-structure system, *Journal of Sound and Vibration* 187 (4) (1995) 695–712.
[30] R. Walther, B. Houriet, W. Isler, P. Mota, *Cable Stayed Bridges*, Thomas Telford Ltd., 1999.